Ground-based measurements of UVB in Namibia

P.F. Cunningham[a*] and G.E. Bodeker[b]

THE FIRST GROUND-BASED MEASUREments of surface erythemal (sunburn-causing) UV irradiances at a number of locations in Namibia are reported. The data for the spring and summer of 1999 and early 2000 show UV indices of up to 20. In addition to downwelling irradiances, upwelling irradiances were measured indicating reflectivity values in excess of 12% on the dry Etosha Pan. Airborne measurements made over the pan and the adjoining surfaces indicate an influence scale length of over 30 km. The seasonal behaviour in erythemal irradiance is consistent with radiative transfer model predictions. The absence of any statistically verifiable trend in 21 years of satellite-based total column ozone over Namibia suggests that unless there have been long-term changes in cloud cover, the measurements reported here may be representative of recent decades.

Studies of the reduced ozone layer, in particular over the poles,[1,2] have caused concern over levels of ultraviolet (UV) radiation. Studies indicate an anti-correlation between ozone thickness and skin cancer.[3] Recently developed algorithms[4] that make use of satellite-based measurements of total column ozone (to infer the clear-sky surface irradiance) and reflectivity (to infer the perturbation to the clear-sky irradiance by clouds) can estimate surface erythemal irradiance. Ground-based measurements are still indispensable for routine daily monitoring, however, since they provide measurements of the changing surface irradiance throughout the day rather than a spot measurement at the time of the satellite overpass. Furthermore, satellite retrievals of UV measurements are spatially averaged, which may not be representative for a fixed location within the satellite's field of view in the presence of scattered clouds.

Extensive measurements of UV radiation have been made in South Africa.[5] However, in places like Namibia situated farther north in the tropics, UV is likely to be different due to smaller summer-time solar zenith angles (SZA is the angle from the direction of the sun to the vertical), generally less cloud cover and reduced ozone absorption. Furthermore, the population in Namibia is small and one may expect lower atmospheric turbidity (and hence higher UV) from activities such as biomass burning.

Measurements of erythemally-weighted UV integrated over the range 280–320 nm were made using a YES UVB pyranometer,[6] which records incident irradiance over 2π steradians. It was thus operated with a full view of the horizon. Data were taken every 15 s and averaged every minute. The data were first corrected for instrument angular sensitivity (cosine response) and then weighted with a Diffey erythemal action spectrum.[7] The UV index is calculated by dividing the values in mW m^{-2} by 25. In this paper, we report daily peak values only. Total column ozone values used in this article are from the NASA TOMS instruments flown on the Nimbus 7,[8] Meteor 3,[9] Earth Probe[10] and Adeos[11] satellites and from the Global Ozone Monitoring Experiment (GOME) flown on ERS-2.[12] Data for specific locations were extracted from the 1° latitude × 1.25° longitude gridded satellite data using bilinear interpolation. The satellite's orbits result in sampling every 24 hours for TOMS and every 72 hours for GOME, close to local midday.

The spring and summer daily peak UV indices for a number of locations in Namibia are shown in Fig. 1. Routine monitoring takes place in Windhoek (latitude 22.6°S) at the University of Namibia, but measurements are also taken at other locations on occasions.

UV indices up to 20 were calculated. These values are high compared to maximum values of 14 reported at Durban.[5] The smaller midday SZA over locations in the tropics cause a reduced path though the ozone layer that results in less UV absorption. Furthermore, as shown by LIDAR studies,[13] the city of Windhoek, which is situated at an altitude of 1800 m, could have up to 5% less total column ozone compared with locations at similar latitudes at sea level, owing to the reduced path length through the troposphere.

It is noticeable that the highest values of midday UV were measured during January and February in comparison with measurements made in Durban,[5] which show a decrease from early January. This is not unexpected, since the SZA in Namibia decreases again as the relative path of the sun travels north. The results of calculations made from a radiative transfer model[14,15] for clear-sky conditions are also shown in the figure. Monthly-averaged TOMS and GOME total column ozone data were input as a main parameter. Although lacking a complete transient meteorological and atmospheric profile, the seasonal behaviour is consistent with experimental values. A clear-sky campaign data point for the relatively populated area of Rundu (latitude 17.9°S) is included in the figure.

Figure 1 also shows UV data from Okaukuejo, situated on the southern shore of Etosha Pan (latitude 18.8°S). The days chosen in November and January coincided with the periods of zero midday SZA. Figure 2 shows the monthly averaged total column ozone values for 1999 and early 2000 taken from the Earth Probe TOMS instrument. It can be seen that there is a peak around October. This results from the annual cycle in southern hemisphere stratospheric dynamics associated with the formation of the Antarctic

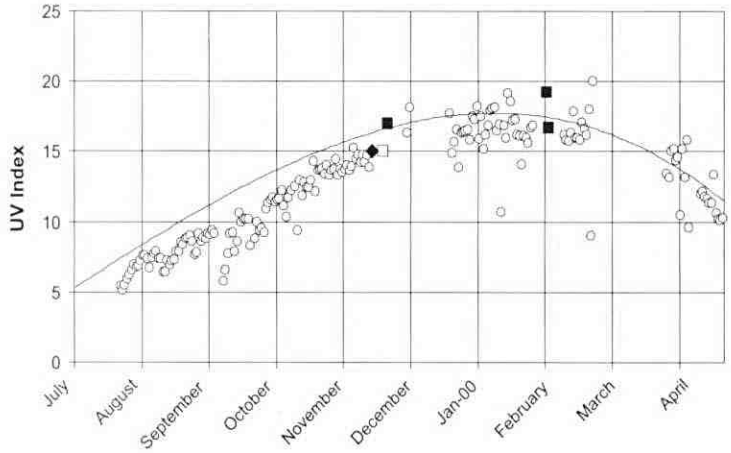

Fig. 1. Peak midday UV Index values. ○ Windhoek, ■ Okaukuejo Etosha, ◆ Rundu. Solid line is from calculations of UV radiation transfer model.[14]

[a]Physics Department, University of Namibia, Private Bag 13301, Windhoek, Namibia.
[b]National Institute of Water & Atmospheric Research, Lauder, Central Otago, New Zealand.
*E-mail: pcunningham@mail.unam.na

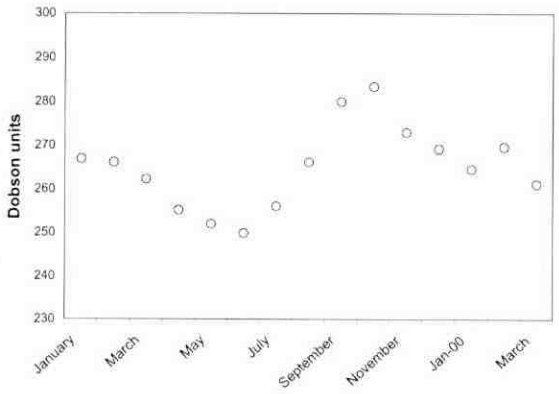

Fig. 2. Monthly averaged total column ozone values for Windhoek from January 1999 to March 2000.

circumpolar vortex and the concomitant accumulation of ozone northwards of the vortex edge. This elevates ozone levels over the hemisphere outside the vortex. This buildup of ozone, although less in Namibia than farther south in South Africa, would partly explain the lower UV indices in November compared with January. Another factor is the high atmospheric turbidity present before the rainy season, which started in December.

The measurements taken at Okaukuejo were also compared with those predicted from the UV radiative transfer model. In this case TOMS daily total column ozone values were used. The predicted and actual data were comparable to within an error in UV index of ±2 for clear-sky conditions and the model predicted the observed increase of UV from November to January. Reducing the parameter of lower level aerosols by 50% for January because of the rain increased the predicted UV index by only 1, which is smaller than the model predicting error.

Reflectivity values were taken on and off the Etosha Pan during the dry pre-rain period in November and again after substantial rains in January. Values were obtained by simply inverting the pyranometer for periods of several minutes at midday and dividing by interpolated incident data. The values are tabulated below.

	On the pan	1 km inland from shore
November	12%	11%
January	3%	4%

It was noticeable that the normally whitish surface of the pan remained significantly greyer for periods of several days after the rain, resulting in a lower reflectivity. The area studied inland of the shore was significantly more vegetated in January, thus reducing the cross-section of exposed dust, causing a similar drop in reflectivity. These high reflectivity values are not inconsistent with measurements of between 10% and 15% reported over limestone.[16]

Mounting the YES instrument on the roof of a small aircraft enabled us to test the short-range influence of the pan. Data were taken as the aircraft flew from some 30 km out towards and across the shore of the pan. The effect of rising UV values as a result of the increasing SZA during the flight was allowed for by comparing with data taken at identical SZAs during clear-sky conditions at a fixed location on the Okaukuejo airstrip a few days earlier. The results show no significant change above the normal variations in the data series, implying an influence scale length of more than 30 km.

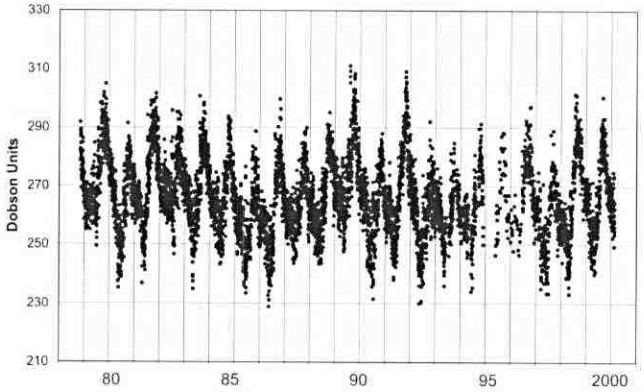

Fig. 3. Daily total column ozone values (Dobson units) for Windhoek from November 1978 to March 2000.

Figure 3 shows the daily TOMS/GOME total column ozone values recorded from late 1978 to May 2000. This series extends data published from Nimbus-7 TOMS from 1978 to 1992.[17] A regression analysis test at the 5% level indicates no significant decline in the yearly means over the last 20 years. This is consistent with recent predictions of UV trends for South Africa.[18]

In summary, the first ground-based measurements of UVB in Namibia made with the widely used YES UVB-pyranometer are reported. High values of the UV index of up to 20 were calculated for a number of places during periods of peak radiation, especially between December and March. Values above 10 are regarded as high. High reflectivity values of up to 12% were measured on the Etosha Pan and will increase UV levels by secondary scattering. This effect may be harmful to people living up to several tens of kilometres from the edge of the pan. Data from the NASA satellite total-column-ozone programme specific to Namibia are also reported here. Because there has been no statistically confirmed decrease in ozone over the last twenty years and since the ozone layer thickness is a major influence on surface UV, it is possible that the levels reported here have been present over the past two decades.

We acknowledge with thanks the assistance provided by the staff at the Etosha Ecological Institute and N.O. Ama and M. Muller of the Statistics Department, University of Namibia.

Received 22 June. Accepted 28 September 2000.

1. Farman J.C., Gardiner B.G. and Shanklin J.D. (1985). Large losses in ozone in Antarctica reveal seasonal ClO_x/NO_x interaction. *Nature* **315**, 207–210.
2. World Meteorological Organization (1999). Scientific assessment of ozone depletion: 1998, global ozone research monitoring project. Rep. 44. WMO, Geneva.
3. UNEP (1996). *Ozone in action*. Ozone Secretariat, United Nations Environment Programme, Nairobi.
4. Eck T.P., Bhartia P.K. and Kerr J.B. (1995). Satellite estimation of spectral UVB irradiance using TOMS derived total ozone and UV reflectivity. *Geophys Res. Lett.* **22**, 611–614.
5. Duigan B.L., Scourfield M.J.W. and Stefanski B. (1995). Surface UVB irradiance measurements at Durban during 1993. *S. Afr. J. Sci.* **91**, 394–398.
6. Dichter B.K., Beaubian A.F. and Beaubian D.J. (1993). Development and characterisation of a new solar ultraviolet-B irradiance detector. *J. Atmos. Oceanic Tech.* **10**, 337–344.
7. McKinlay A.F. and Diffey B.L. (1987). A reference spectrum for ultraviolet-induced erythema in human skin. In *Human Exposure to Ultraviolet Radiation: Risks and Regulations*, eds W.R. Passchler and B.F.M. Bosnajokivoc. Elsevier, Amsterdam.
8. McPeters R.D., Bhartia P.K., Krueger A.J., Herman B.M., Schlesinger B.M., Wellemeyer C.G., Seftor C.J., Jaross G., Taylor S.L., Swissler T., Torres O.,

Labow G., Byerly W. and Cebula R.P. (1996). Nimbus-7 Total Ozone Mapping Spectrometer (TOMS) Data Products User's Guide, NASA Ref. Pub. No. 1384 (PDF file available on http://toms.gsfc.nasa.gov/).
9. Herman J.R., Bhartia B.K., Krueger A.J., McPeters R.D., Wellemeyer C.G., Seftor C.J., Jaross G., Schlesinger B., Torres O., Labow G., Byerly W., Taylor S.L., Swissler T., Cebula R.P. and Gu X. (1996). Meteor-3 Total Ozone Mapping Spectrometer (TOMS) Data Protocol User's Guide, NASA Ref. Pub. No. 1393 (PDF file available on http://toms.gsfc.nasa.gov/).
10. McPeters R.D., Bhartia P.K., Krueger A.J., Herman J.R., Wellemeyer C.G., Seftor C.J., Jaross G., Torres O., Moy L., Labow G., Byerly W., Taylor S.L., Swissler T. and Cebula R.P. (1998). Earth Probe Total Ozone Mapping Spectrometer (TOMS) data products user's guide, NASA Ref. Pub. (PDF file available on http://toms.gsfc.nasa.gov/).
11. Krueger A.J., Bhartia P.K., McPeters R.D., Herman J.R., Wellemeyer C.G., Jaross G., Seftor C.J., Torres O., Labow G., Byerly W., Taylor S.L., Swissler T. and Cebula R.P. (1998). ADEOS Total Ozone Mapping Spectrometer (TOMS) Data Products User's Guide, NASA Ref. Pub. (PDF file available on http://toms.gsfc.nasa.gov/).
12. Burrows J.P., Weber M., Buchwitz M., Rozanov V., Ladstätter-Weissenmayer A., Richter A., DeBeek R., Hoogen R., Bramstedt K., Eichmann K-U. and Eisinger M. (1999). The Global Ozone Monitoring Experiment (GOME): mission concept and first scientific results. *J. Atmos. Sci.* **56**, 151–175.
13. Beekmann M.G., Ancellet G., Megie G., Smit H.G.J. and Kley D. (1994). Intercomparison campaign of vertical ozone profiles including electrochemical sondes of ECC and Brewer-Mast type and a ground based UV differential absorption lidar. *J. Atmos. Chem.* **19**, 259–288.
14. Green A.E.S., Mo T. and Miller J.H. (1974). A study of solar erythemal radiation doses. *Photochemistry and Photobiology* **20**, 473.
15. 'UV-Calc'© (1996). Yankee Environmental Systems Inc., info@yesinc.com
16. Blumthaler M. (1993). Solar UV measurements. In *UV-B Radiation and Ozone Depletion*, ed. M. Teveni, pp. 71–94. Lewis, Florida.
17. Cunningham P.F. (1998). The behaviour of the ozone layer above tropical southern Africa. *Trans. Zimbabwe Sci. Soc.* **72**, 14–17.
18. Bodeker G.E. and Scourfield W.J. (1998). Estimated past and future variability in UV radiation in South Africa based on trends in total column ozone. *S. Afr. J. Sci.* **94**, 24–32.

Existence of covalently cross-linked haemoglobin in human erythrocytes, and its induction by naturally occurring sugars *in vitro*

P.A. Berman[a]* and W.F. Brandt[b]

NON-ENZYMATIC GLYCOSYLATION OF proteins is a major contributor to the pathology of diabetes, ageing, and neurodegenerative disease. Advanced glycosylation end-products (AGEs) so formed are chemically heterogeneous, but typically include intermolecular protein crosslinks. We report here the presence of covalently cross-linked haemoglobin monomers in red cells of healthy subjects. Dimers are of predicted size on SDS/polyacrylamide gel electrophoresis, react with anti-haemoglobin antibodies in Western blots, and display N-terminal sequence consistent with an equal mixture of α- and β-globin subunits. Incubation of red cell lysates with naturally occurring sugars accelerates formation of globin dimers and higher-order oligomers. Crosslinking potency is highly variable among the sugars tested, with a rank order of glucose < fructose < ribose, and phosphorylated sugars being more potent than their unphosphorylated counterparts. Aminoguanidine, a pharmacological inhibitor of AGE formation, strongly inhibits crosslinking by preventing sugar binding to haemoglobin, but is unable to dissociate pre-formed crosslinks. This is, to our knowledge, the first report of cross-linked haemoglobin occurring *in vivo*, and catalysis of its formation by sugars *in vitro*.

Departments of Chemical Pathology[a] and Biochemistry[b], University of Cape Town, Medical School, Observatory, 7925 South Africa.
*Author for correspondence.
E-mail: pete@chempath.uct.ac.za

Progressive non-enzymatic modification of tissue macromolecules by glucose has been implicated in the pathogenesis of a variety of disorders, including ageing and the long-term complications of diabetes.[1,2] It begins with reversible attachment of glucose to free amino groups on proteins, forming a Schiff base, which subsequently undergoes Amadori rearrangement to a more stable ketoamine. Further chemical modification of the ketoamine, including dehydration, rearrangement and fragmentation, ultimately yields a biochemically heterogeneous collection of sugar-modified proteins, termed advanced glycosylation end-products (AGEs), that represent tissue damage at the molecular level. A feature of AGEs is the presence of protein crosslinks, in which an initially glycosylated protein reacts with a labile amino group on a neighbouring protein, forming an intermolecular crosslink.[3] Collagen crosslinks have been implicated in the microvascular complications of diabetes, and chemical cleavage of such crosslinks with a novel agent has proven beneficial effect in a rodent model of diabetes.[4] The importance of AGEs is underscored by the ability of aminoguanidine, a pharmacological inhibitor of the AGE pathway, to retard some,[5–8] but not all,[9] of the long-term complications of diabetes in animal models, and is currently undergoing evaluation in humans. Aminoguanidine, an analogue of the side chain of arginine, is believed to trap post-Amadori glycosylation adducts and prevent development of AGEs.

In contrast to biochemical markers of collagen modification,[5] which require invasive sampling, haemoglobin is readily accessible for analysis, and has been widely used as a model to study protein modification by glucose *in vivo*. For example, haemoglobin A_{1C}, a haemoglobin A variant with a glucose adduct on the N-terminal valine of its β-globin subunit, has found widespread clinical use as an indicator of long-term glycemic control in diabetics. More advanced modification of haemoglobin by glucose, termed haemoglobin-AGE, has also been identified in circulating human erythrocytes, using an ELISA approach. Haemoglobin-AGE content of red cells is increased in diabetics, and correlates with levels of HbA_{1C}.[10] It falls in parallel with HbA_{1C} in diabetics subjected to stricter control of blood glucose.[11] Aminoguanidine retards glucose-induced haemoglobin-AGE formation *in vitro* by >95%, but is unable to reverse it.[10]

Haemoglobin consists of a non-covalently bound tetramer of two α- and two β-globin subunits, which dissociate in sodium dodecylsulphate (SDS) into monomers of 141 and 146 amino acids, respectively. These migrate on denaturing polyacrylamide gel electrophoresis (PAGE) as a single band of approximately 16 kDa. Covalent intermolecular crosslinks should be readily apparent as additional higher molecular weight bands integral multiples of 16 kDa. In this study, we adopt an electrophoretic approach to investigate the presence of haemoglobin crosslinks *in vivo*, and their induction by naturally occurring sugars *in vitro*.

Demonstration of haemoglobin dimer, and its induction by sugars

Figure 1A shows a human red cell lysate incubated for 48 h with various sugars, then analysed by denaturing SDS/PAGE and stained with Coomassie blue. Haemoglobin monomer, moving as a 14 kDa band, is the predominant protein in all samples. The second most abundant protein is approximately 28 kDa, consistent with covalently linked haemoglobin dimer. While its presence is not sugar dependent, its intensity is appreciably enhanced by certain sugars. Glucose and fructose have negligible effect, whereas their phosphorylated forms, glucose-6-phosphate (G-6-P) and fructose-6-